Biophysical Journal, Volume 97

Supporting Material

Polymorphism of Alzheimer's Aβ17-42 (p3) Oligomers: The Importance of the Turn Location and its Conformation

Yifat Miller, Buyong Ma, and Ruth Nussinov

Supporting Material – Figure legends:

Fig. S1: Total energy during time of simulations of single layer $A\beta_{17-42}$ oligomers for models M1 and M2.

Fig. S2: Total energy during time of simulations of double layer $A\beta_{17-42}$ oligomers for models M4 and M5.

Fig. S3: Initial structural models of antiparallel $A\beta_{17-42}$ oligomers for Lührs' model, viewed from top: (A) Single layer, model M7 (B) Double layer, model M8 (C) Single layer, model M12.

Fig. S4: Initial structural models of antiparallel $A\beta_{17-42}$ oligomers for Tycko's model: (A) Single layer, model M9, viewed from side (B) Single layer, model M9, viewed from top (C) Single layer, model M13, viewed from top (D) Single layer, model M14, viewed from top (E) Single layer, model M14, viewed from side.

Fig. S5: Initial structural models of antiparallel $A\beta_{17-42}$ oligomers for Ma-Nussinov's model: (A) Single layer, model M10, viewed from top (B) Double layer, model M11, viewed from side.

Fig. S6: RMSDs of single-layered $A\beta_{17-42}$ oligomers for Tycko's model (M1) and Lührs' model (M2): (A) for full-segment (two β strands and U-turn) (B) for U-turn region (residues 22-29).

Fig. S7: The averaged distance between Cα of Asp23 and N of Lys for single-layered $A\beta_{17-42}$ oligomers for (A) Tycko's model (M1) and for (B) Lührs' model (M2).

Fig. S8: RMSDs of double-layered $A\beta_{17-42}$ oligomers for Tycko's model (M3) and Lührs' models (M4 and M5): (A) for full-segment (two β strands and U-turn) (B) for U-turn region (residues 22-29).

Fig. S9: The averaged distance between Cα of Asp23 and N of Lys for double-layered $A\beta_{17-42}$ oligomers for (A) Tycko's model (M3) and for (B) Lührs' model (M4).

Table S1: Various types of polymorphism and related models

Text 1: Detailed Generalized Born Method with Molecular Volume (GBMV) calculations.

Text 2: Details for the definition of the core domain

Fig. S1

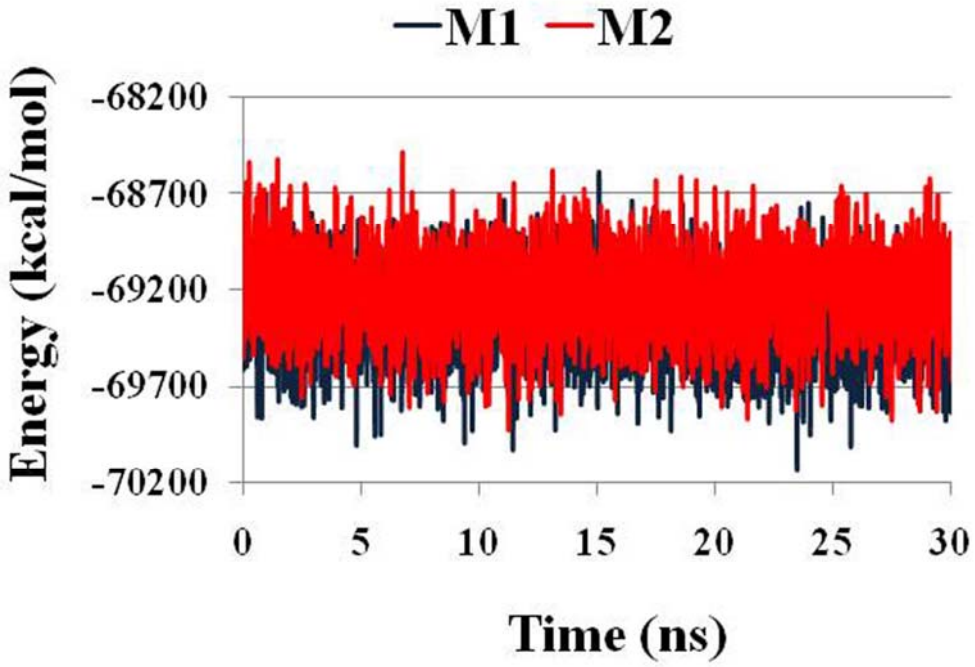
M1
M2
Energy (kcal/mol)
-68200
-68700
-69200
-69700
-70200
0
5
10
15
20
25
30
Time (ns)

Fig. S2

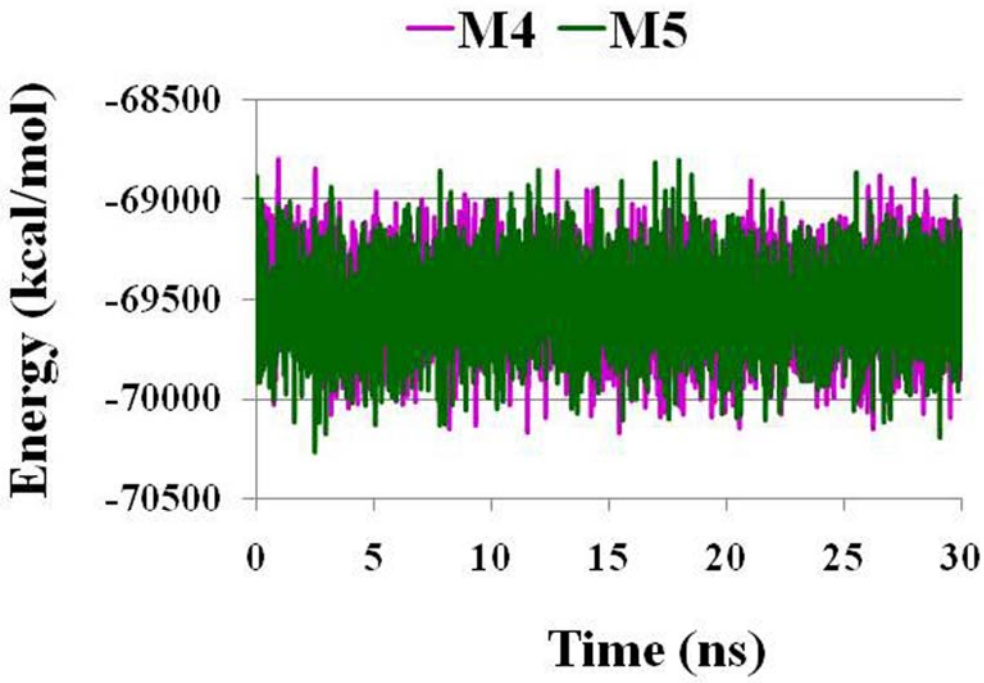
M4
M5
Energy (kcal/mol)
-68500
-69000
-69500
-70000
-70500
0
5
10
15
20
25
30
Time (ns)

Fig. S3

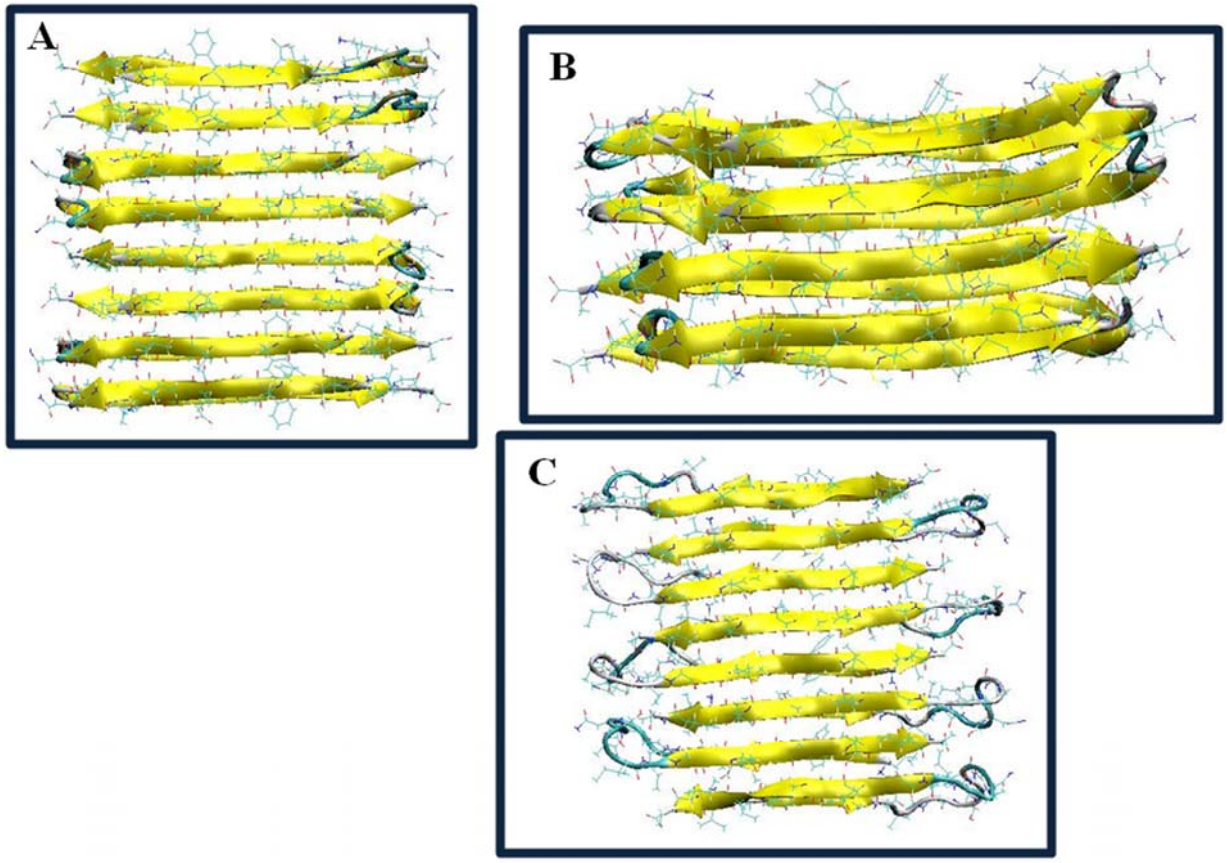

Fig. S4

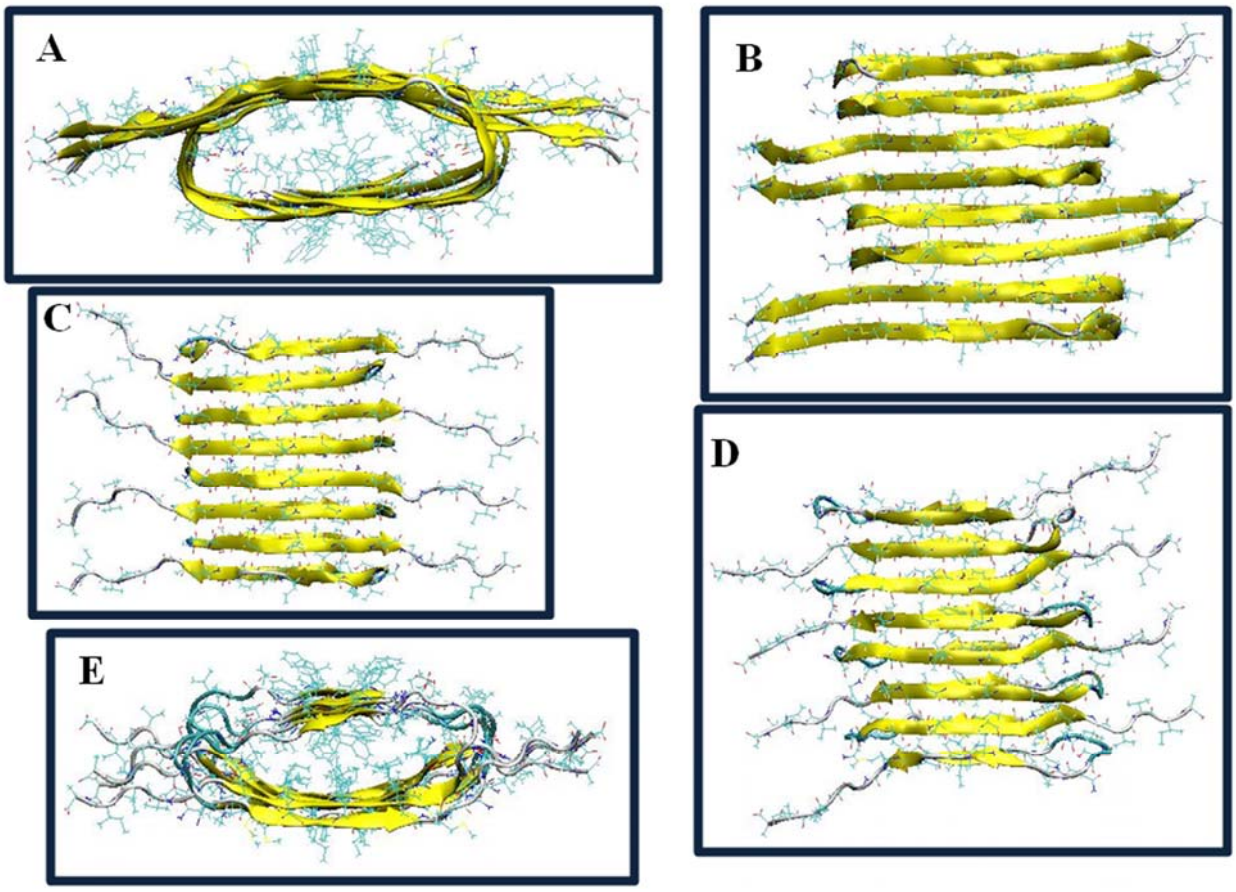

Fig. S5

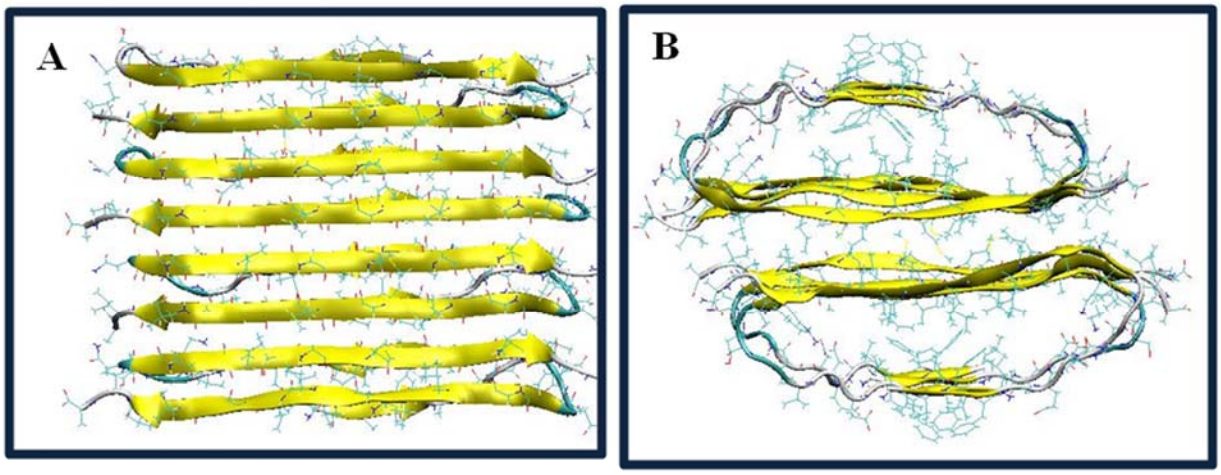

Fig. S6

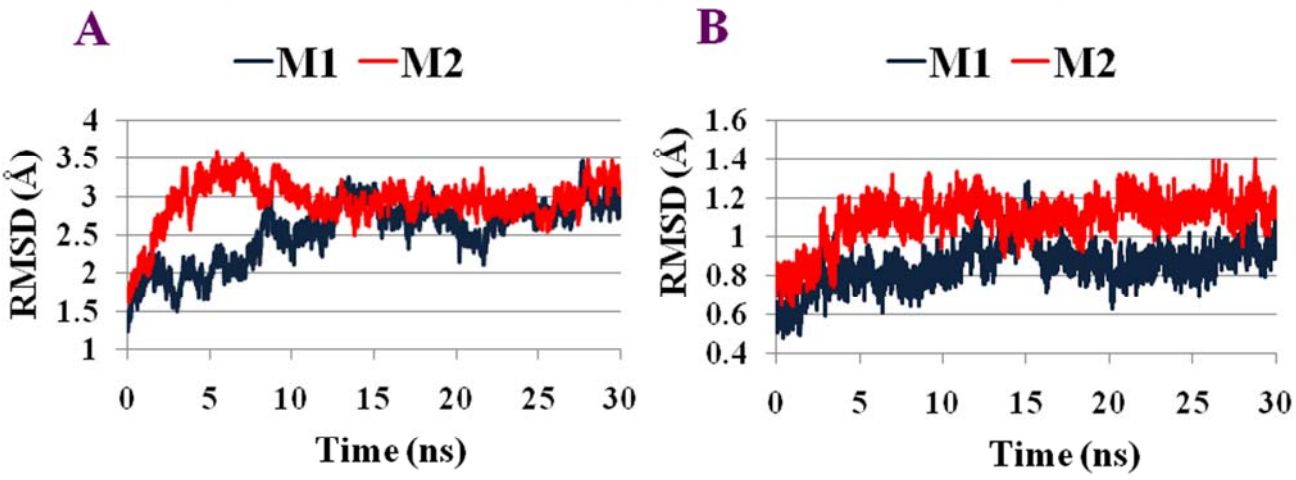
A
M1
M2
RMSD (Å)
4
3.5
3
2.5
2
1.5
1
0
5
10
15
20
25
30
Time (ns)
B
M1
M2
RMSD (Å)
1.6
1.4
1.2
1
0.8
0.6
0.4
0
5
10
15
20
25
30
Time (ns)

Fig. S7

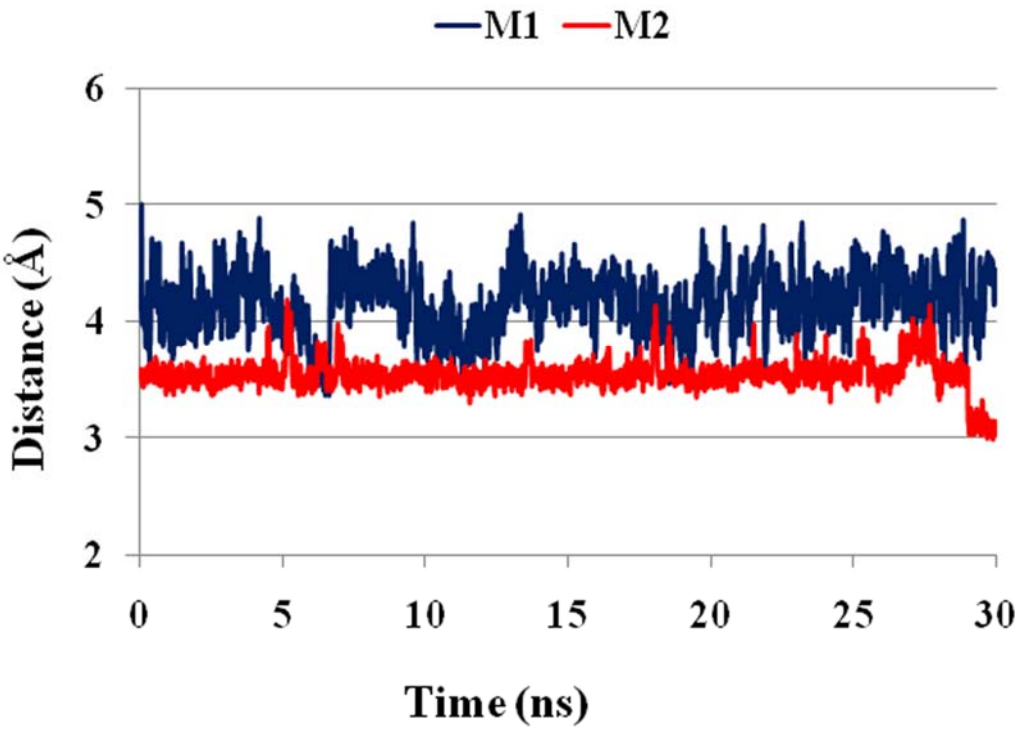

Fig. S8

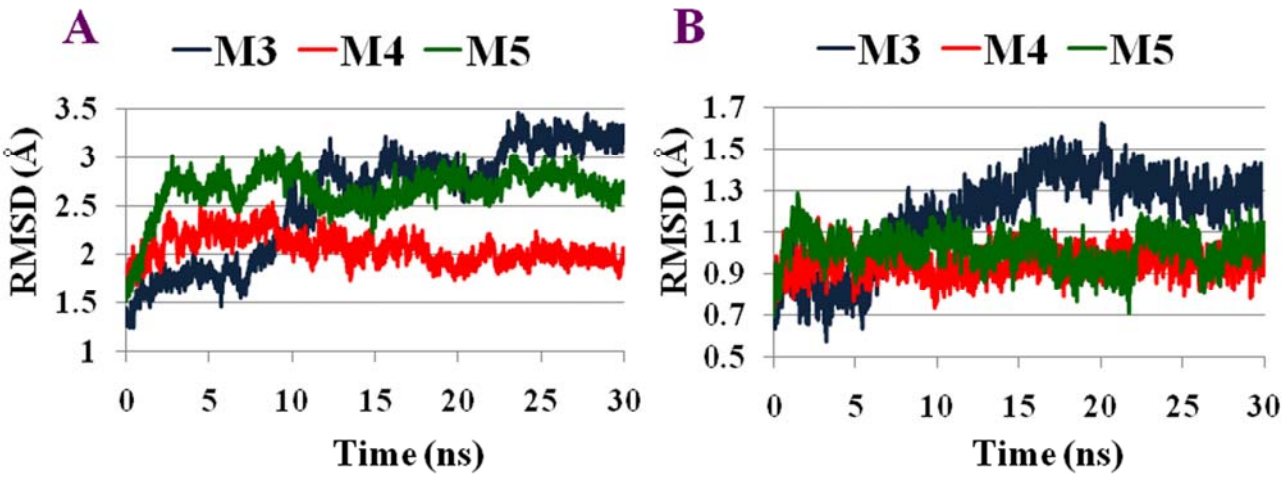
A
M3 M4 M5
RMSD (Å)
3.5
3
2.5
2
1.5
1
0 5 10 15 20 25 30
Time (ns)
B
M3 M4 M5
RMSD (Å)
1.7
1.5
1.3
1.1
0.9
0.7
0.5
0 5 10 15 20 25 30
Time (ns)

Fig. S9

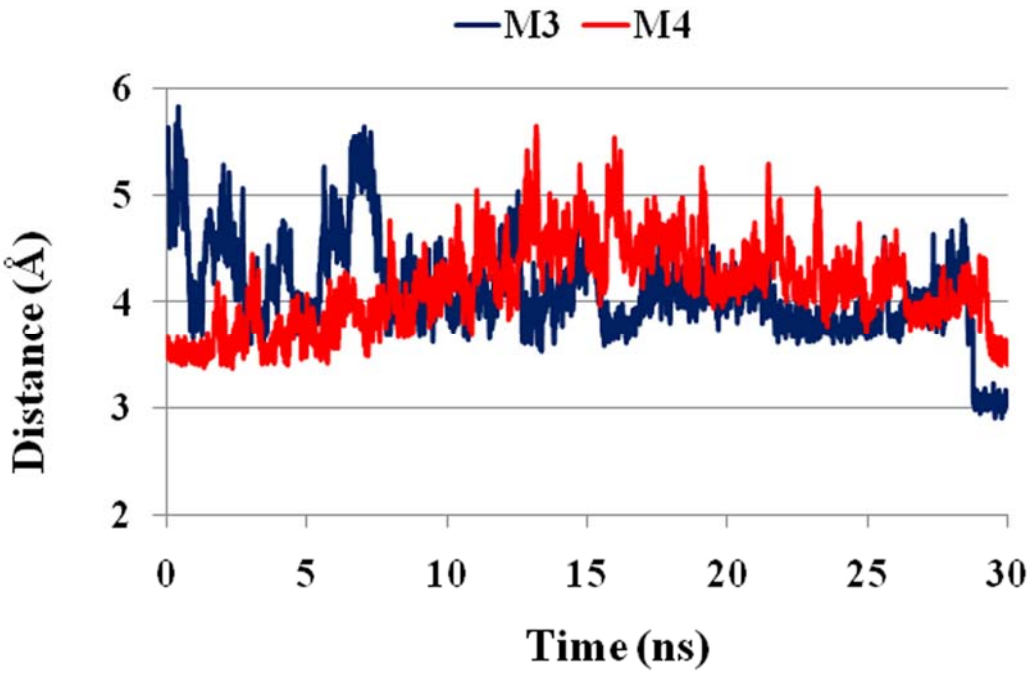

Table S1:

Type of polymorphism	**Alignment of β-strand (single layer)**	**Backbone U-turn conformation**	**Assignment of β-sheets (double layer)**
Conformers to compared	M1/M2 M7/ M9 M10/ M12/ M13/M14	M1/M2, M3/M4 M10/M12/M13	M4/M5/M6
Favorable conformers	M1,M2	M1, M2 M3, M4	M4, M5

Text 1:

Generalized Born Method with Molecular Volume (GBMV)

In the GBMV calculations, the dielectric constant of water was set to 80.0 and no distance cutoff was used. The hydrophobic solvent-accessible surface area (SASA) term factor was set to 0.00592 kcal/mol·Å^2. Each conformer is minimized using 1000 cycles and the conformational energy is evaluated by grid-based GBMV. The minimization does not change the conformations of each conformer, only relaxing the local geometries due to thermal fluctuation which occurred during the MD simulations.

A total of 7000 conformations (500 conformations for each of the 14 conformers examined) were used to construct the effective energy landscape of the $A\beta_{17-42}$ oligomer and to evaluate the conformer probabilities by using Monte Carlo (MC) simulations. We note that using more or less conformations than used here would not change the conformer probabilities. At the first step two conformations i and j are randomly selected from the conformational ensemble. The Boltzmann factor is then computed as $e^{-(Ej - Ei)/KT}$, where E_i and E_j are the conformational energies evaluated using the GBMV calculations for conformations i and j, respectively, K is the Boltzmann constant and T is the absolute temperature (298 K used here). If the Boltzmann factor value is larger than the random number, the move from conformation i to conformation j is allowed. After 1 million steps, the conformations visited for each conformer were counted. Finally, the relative probability of conformer n was evaluated as: $P_n = N_n / N_{total}$, where P_n is the population of conformer n, N_n is the total number of conformations visited for the conformer n, and N_{total} is the total steps. The advantages of using the MC simulations to estimate conformer probability rely on the facts that the MC simulations have good numerical stability and allow transition probabilities among several conformers to be controlled. We use both the averaged energies and the more accurate calculation of the populations obtained from the MC procedure to show the similarities and differences among the various arrangements. Both are reported for comparison.

Text 2:

Details for the definition of the core domain

The core domain is defined as the Cα backbone-backbone distance close to the salt bridge of each model. The core domain for each model is different due to the different U-turn locations. In Lührs' model the Cα backbone-backbone distance is between Glu22-Met35 and in Tycko's model it is between Ala21-Ile31. We calculated the C_α distances for all peptides within an oligomer, and used the averaged values for the C_α distances within the oligomer.